SLAC–PUB–14399

Tracking Study for Top-off Safety Validation at SSRL

Xiaobiao Huang, Johannes Bauer, Jeff Corbett, Deminico Dell'Orco, Bob Hettel, James Liu, Tom Rabedeau, James Safranek, John Schmerge, Jim Sebek, Jack Tanabe, Andrei Terebilo, Lanfa Wang

SLAC National Accelerator Laboratory, 2575 Sand Hill Road, Menlo Park, CA 94025

Abstract

A tracking study was performed at SSRL to identify necessary controls and to prove the safety of top-off operation from radiation hazard under such conditions. The safety rationale, tracking setup and the results are presented.

Keywords: top-off, injection, SPEAR3

1. Introduction

Top-off operational mode has become a trend for existing and planned third-generation storage ring light sources for the many benefits such as increased average brightness, improved thermal stability and elimination of the interruption to user experiments due to traditional injection [1, 2]. Unlike the traditional decay mode injection which happens a few times a day and during which the photon beamline shutters are closed, top-off mode injection requires photon beamline shutters to remain open during injection and occurs much more frequently, from once every 5 seconds to once every 30 minutes. Therefore injection may be transparent to user experiments and the stored current variation can be significantly reduced.

For a facility equipped with a full-energy injector, the biggest challenge to the implementation of the top-off mode may be the control of radiation hazard. Studies at ALS and SSRL [2, 3] have shown that a single injected electron pulse that enters the photon beamline and exits the radiation shield wall would cause unacceptable radiation doses on the experimental floor. For

Email address: xiahuang@slac.stanford.edu (Xiaobiao Huang)

Work supported in part by US Department of Energy contract DE–AC02–76SF00515.

the protection of users and experimental equipment, it is hence a prerequisite for top-off operation to establish controls that absolutely prevent such occurrences.

Similar to other facilities such as ALS and APS [2, 4], tracking simulations were conducted at SSRL to identify the control measures, define the specifications and prove the radiation safety. However, a different approach toward the proof of safety is taken at SSRL. In this paper we first describe the SSRL accelerator complex with emphasis on the aspects related to top-off in section 2. The general considerations and requirements for top-off are presented in section 3. Section 4 and 5 give a detailed description of the tracking setup and results. Concluding remarks are given in section 6.

2. The SPEAR3 storage ring and the injector system

SPEAR3 is a third-generation storage ring light source [5]. It was built inside the same tunnel as its predecessor SPEAR2 and inherited the racetrack shape of the original SPEAR ring. Some basic parameters are shown in Table 1. It consists of 18 double-bend-achromat (DBA) cells, including 14 standard cells and 4 matching cells. The bending angle of the dipole magnets in the matching cells is 3/4 of that of the standard dipoles. There are currently 13 user beamlines, including 4 dipole beamlines and 9 insertion device (ID) beamlines. The dipole beamlines extract synchrotron radiation from the first dipole magnet of the standard DBA cells. Insertion devices for most ID beamlines are placed in standard straight sections, except the undulator of Beamline 13 is in a matching straight section and the in-vacuum undulator of Beamline 12-2 in a chicane straight section inside one of the two long straight sections (the other long straight section is occupied by rf cavities).

The full-energy injector consists of a thermionic rf gun, a 150-MeV linac, a 3-GeV Booster synchrotron and transport lines from the linac to the Booster (LTB) and from the Booster to the storage ring (BTS). The BTS transport line ends at the septum magnet. During injection, the stored beam is brought inward to the septum wall through a closed-orbit bump created by three kickers that are simultaneously fired for a duration of about 1 μsec. The injected beam has an initial horizontal offset of -11.5 mm relative to the stored beam. The horizontal oscillation of the injected beam is damped down in about 5 ms. The injector operates at 10 Hz. The average beam

power through the BTS transport line is limited by an interlock system to be below 5 W.

Table 1: SPEAR3 parameters.

Parameter	value	unit
Circumference	234.1	m
Energy	3	GeV
emittance	10	nm
beam current	500	mA
lifetime	12	hr

3. General safety rationale and considerations for top-off at SSRL

Under normal operation, the total beam loss for the top-off mode is higher than the traditional decay mode because of increased average beam current, increased beam loss rate and increased injection losses. However, for SPEAR3, the average beam power loss is estimated to be low. Even for 500 mA operation, it is on the order of 2 mW at locations of limiting apertures [6]. Therefore the primary safety concern is the abnormal beam loss scenarios in which the injected electrons exit the SPEAR vacuum chamber, enter the photon beamline and potentially exit the SPEAR concrete tunnel (the ratchet wall).

There is a hierarchy of accelerator safety systems preventing such scenarios from happening. The beam shut-off ionization chamber (BSOIC) system can shut beam off upon detection of abnormal radiation activities. The fast orbit feedback system maintains the closed orbit accurately, to a level of a few microns. The orbit interlock system interlocks the closed orbit position and angle at the insertion device straight sections which would dump the beam within a few milliseconds when a violation is detected. With the stored beam on the normal orbit, the injected beam needs to be significantly mis-steered to enter the photon beamline, if the apertures inside the SPEAR vacuum chamber do not intercept such a trajectory. The likelihood of the abnormal beam loss hazard is very low under normal operation condition.

However, as no chance can be taken when safety is concerned, it is necessary to identify all conditions under which the injected beam may enter

the photon beamline. This is done by tracking simulations and is the main topic of the present paper. An independent interlock system needs to be set up to prevent such conditions from occurring during top-off operation. The conditions cover any machine and beam parameter that affects the trajectory of the injected beam, for example, the injected beam energy, SPEAR power supply failures and SPEAR magnet shorts. The new top-off interlock system provides a new layer of protection.

New radiation monitors are also set up for each beamline. In the very unlikely event when the machine enters an abnormal state and simultaneously the injected beam is mis-steered and both the top-off interlock system and the original beam containment interlock system fail, these radiation monitors and the BSOIC system serve as the last line of defense. Analysis has shown that if in an accident the injected beam reaches the experimental floor, it will be terminated in time to limit the integrated dose to ~ 90 mrem [3], much below the accident scenario limit.

4. The general tracking approach and the standard ID beamline case

The purpose of the particle tracking study is to identify the abnormal conditions under which a mis-steered injected beam can potentially enter the photon beamline and pass beyond a certain *safe endpoint*, define specifications for the interlocks that are designed to prevent such conditions, and prove that within the interlock limits no electrons can pass beyond the safe endpoint. The safe endpoint for each beamline is usually defined as a radiation mask upstream of the ratchet wall.

The general approach taken in this study is *forward tracking*. Particles with all possible initial coordinates are launched at one point in the storage ring to simulate the injected beam. The particles are transported downstream through various accelerator elements, such as drift spaces and magnets. At the location of a controlled aperture, particles that exceed the aperture limits are removed. Finally at the safe endpoint the positions of the particles are examined.

Since usually there is no magnetic field in the photon beamlines, particle tracking is needed only for a section of the storage ring. According to the structures of the accelerator sections that are involved in the tracking study, all the SPEAR3 beamlines fall into one of the four cases: the standard

straight section ID beamlines, the dipole beamlines, Beamline 12 and Beamline 13. In this section we use the standard ID beamline case to illustrate our general tracking approach.

4.1. Tracking setup

Figure 1 shows the layout of the accelerator and photon beamline sections relevant to the standard ID beamline case. The starting point is the radiation mask (aperture A1) upstream of the insertion device. Particle tracking ends at the exit of the first sextupole magnet after the dipole because the downstream magnets are too far off from the photon beamline to affect the trajectories of electrons in the photon beamline. In addition to the initial position and angle coordinates, the final position and angle coordinates of particles depend on the following factors: (1) the energy of the particles; (2) the magnetic field in the magnets; (3) the apertures in the accelerator section.

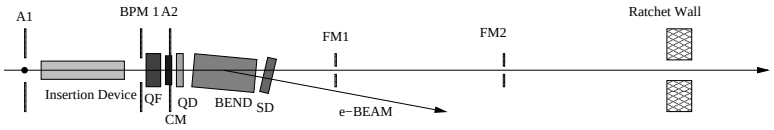

Figure 1: Schematic of tracking setup for the standard straight section ID beamlines.

Higher energy particles are more likely to escape to the photon beamline because they are less contained by the bending magnets. The injected beam energy is limited to be below 3.3 GeV, or 110% of the nominal energy by an active interlock system that interlocks the current of the bending magnets in the BTS transport line [7].

4.1.1. Apertures

Apertures in the storage ring that are credited are located at the radiation mask preceding the insertion device (A1), the first beam position monitor (BPM) after the insertion device and the sock mask (A2) inside the corrector magnet. The negative limits of the apertures are the inner wall of the SPEAR3 vacuum chamber, which is -42 mm from the electron beam centerline. The positive limit of the A2 aperture is $+50$ mm. The combined worst case fabrication and alignment tolerance is 1.2 mm. To be conservative, an error tolerance of 5 mm is added to all aperture limits.

The photon beamline apertures vary by the beamlines. For each beamline, two apertures are of importance, one is the safe endpoint, the other is the ratchet wall aperture. The combined tolerance from manufacturing, fiducialization and alignment errors is below 1.6 mm for all beamlines. To apply the same conservatism, a 5 mm tolerance is applied in the simulation. The ratchet wall aperture tolerance is set to 20 mm, which is also more than three times of the conservative estimate.

4.1.2. Treatment of the vertical plane

Similar to ALS [2], our tracking simulation is limited to the horizontal plane. Only horizontal apertures are taken credited for. Effect of particles off the middle plane is accounted for by tightening the interlock limits for the corresponding magnets. Magnet modeling shows that the maximum deviation of the vertical magnetic field (B_y) between the $y = 0$ and the $y = 8$ mm planes for the dipole magnet is at the edges of the poles and is less than 2%. The maximum deviation for quadrupoles between the $y = 0$ and the $y = 5$ mm is also near the poles and is less than 4%. These deviations are included in the accounting of the allowed parameter range for each magnet types.

4.1.3. Magnetic field maps

All dipole, quadrupole and sextupole magnets are modeled by one-dimensional (1D) $B_y(x)$ field profiles. A hard-edge model is assumed for the longitudinal distribution of fields. It is possible to use two-dimensional (2D) field maps that include longitudinal field roll-off but the tracking speed will be reduced. It has been shown that the 1D model produces more conservative result than the 2D model for the dipole magnets.

The 2D dipole field map on the mid-plane was experimentally measured for a portion of the magnet, including the fringe field region. The field map by the magnet model agrees very well with the measurements. Figure 2 shows the normalized field profile from both the measurement and the magnet model. The field profile extends to large horizontal offset because the electron beam may be severely mis-steered.

There are four types of quadrupoles in SPEAR3 which differ only in the core lengths of the magnets. Magnetic field profile for each type of quadrupoles is obtained by a three-dimensional (3D) magnet model. The normalized field profiles are shown in Figure 3. The actual magnetic field in the magnet is obtained by multiplying the normalized profile by $B\rho K_1$,

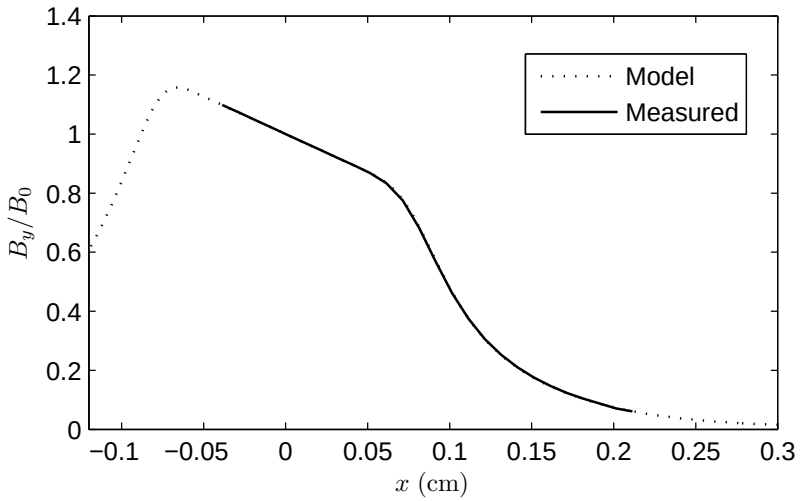

Figure 2: Normalized dipole field map for SPEAR3.

where $B\rho$ is the magnetic rigidity and K_1 the focusing gradient. The focusing gradient is a parameter for the tracking simulation which depends on the nominal value of the magnet and fault scenarios. The three types of quadrupoles in a standard cell are the QF ("34Q"), the QD ("15Q") and the QFC ("50Q") magnets, where the numbers 34, 15 and 50 refer to the approximate magnet lengths in cm.

There are two types of sextupole magnets in SPEAR3. The magnetic field profiles are also obtained with 3D magnet models.

4.1.4. Other magnet models

The corrector magnets, kicker magnets and undulator or wiggler magnets also appear in the accelerator section considered by the tracking simulation. A corrector magnet is modeled as a simple kick. The maximum kick to an electron at the nominal energy is determined by both magnetic field measurement and beam-based calibration. The maximum kick is ± 1.65 mrad for 3 GeV electrons.

Effect of the undulator or wiggler magnets in the straight section is modeled as two kicks to the beam, one at each end of the insertion device. Each kick can be as large as 3 mrad. Analysis has shown that this model is conservative since no existing SPEAR3 ID is capable of supplying such large kicks. The SPEAR3 injection kicker magnets can deliver kicks up to 1.7 mrad. To

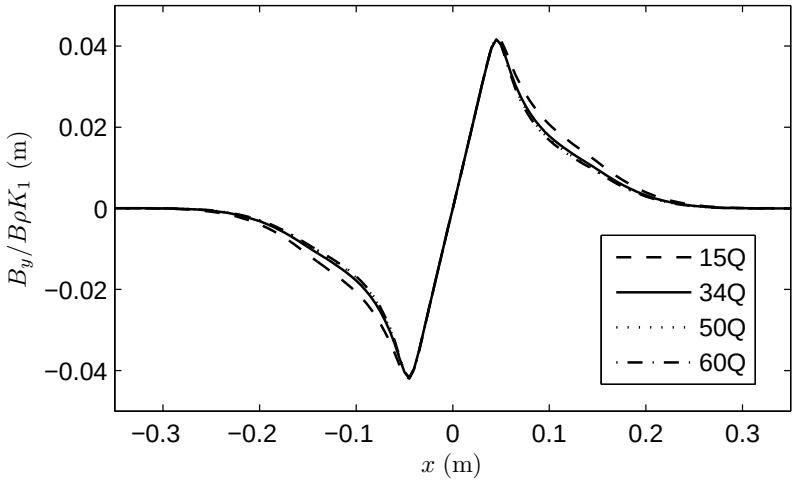

Figure 3: Normalized quadrupole field maps for the four SPEAR3 quadrupole types.

simplify the tracking setup, the total effect of a kicker is modeled in the same manner as the insertion devices, namely two 3 mrad kicks.

4.1.5. Magnet faults

Certain types of magnet failures can cause significant changes to the magnetic field in the magnets and remain undetected, for example, full or partial short of a single coil, external short across power leads on the magnet or short of an entire magnet that cannot be detected by a power supply current interlock. These types of failures rarely happen, usually less than once in the lifetime of the facility. At SPEAR3, we implemented power supply voltage interlocks for all relevant magnets. The voltage interlocks would be able to detect a short in the magnets. We do not consider magnet coil or pole shorts in the tracking simulation.

4.1.6. The tracking code

Simulation in this study is performed within the framework of the accelerator modeling code Accelerator Toolbox (AT) [8]. A new routine was developed to track particles through a vertical magnetic field via numerical integration of the equation of motion. Small angle approximation is not assumed. The routine accepts only horizontal coordinates X and θ. The energy error of the beam is accounted for by scaling the magnetic fields of all mag-

nets simultaneously. The tracking code was verified with two independent codes.

4.1.7. The parameter range

Parameters that affect the injected beam trajectory may vary during operation under both normal or erroneous scenarios. The range of variation for each parameter needs to be defined for the tracking analysis to reach a definitive conclusion. A set of *nominal* values is first defined which represents the machine condition under normal operation. The parameter ranges are defined around the nominal values with the lower and upper limits chosen according to the safety requirements and at the convenience of the implementation of the corresponding controls. As will be explained in the next subsection, within the chosen parameter ranges, the effect of each parameter on the most dangerous trajectory (the extreme ray) and the safety margin is monotonic. Therefore for each parameter the *worst-case* value is either the lower or upper limit, whichever corresponds to an extreme ray that is closer to the experimental floor at the safe endpoint. The nominal values and worst-case values for parameters that are relevant to the standard ID beamline case are shown in Table 2.

Table 2: Nominal and worst-case parameter values for the standard ID beamlines. The worst-case values represent deviations from the nominal values.

Parameter	nominal	worst-case
Injected beam energy	3 GeV	+10%
Bend	1.2389 Tesla	−2.5%
QF	1.75 m^{-2}	−25%
QD	−1.50 m^{-2}	+55%
SD	−21 m^{-3}	+55%
Corrector	0	+1.65 mrad
ID	0	+3 mrad×2

4.2. Tracking analysis

4.2.1. Particle distribution

The actual distribution of the injected beam at the tracking starting point is a complicated function that depends on the initial distribution from the

injector and all magnets in the preceding storage ring section. There is also a possibility that the injected beam circulates one or more turns before reaching an unsafe phase space coordinate. Therefore it is impossible to specify the allowable phase space distribution because too many parameters are involved. This is the reason the forward tracking approach was not preferred at the other labs [2, 4].

In our analysis the initial distribution is chosen to be the phase space area determined by the A1 aperture and a nearby downstream aperture. The two apertures are separated by a short drift space of 0.165 m long. The initial angle coordinate can be as large as 0.8 rad. But since these unrealistic particles will be lost at the next aperture located at BPM 1, they do not cause any difficulty. The way we choose the initial distribution makes our analysis completely independent of the injector and the other parts of the ring except for the energy error of the injected beam. The energy error of the injected beam is mainly affected by extraction timing from the injector and potentially by circulation in the storage ring. The energy error is controlled by an active interlock system in the BTS transport line and it has been proved by simulation that particles cannot accumulate energy error above +10%.

A further simplification is made by tracking only particles on the boundary of the allowed phase space area. This is valid because the coordinate mapping from one location to the next prohibits overlapping of any two phase space points. In a 2D phase space it means particles inside the phase space area will remain within the boundary such that the largest position or angle coordinates are always on the boundary. When the initial phase space boundary is propagated downstream to an aperture, particle on the boundary with position coordinates outside the aperture limits will be removed. To avoid having a gap along the cut-line, new particles are populated on it. Therefore a closed boundary is always maintained.

4.2.2. Extreme ray and safety metric

Figure 4 shows the phase space boundary of the allowed particles at several locations along the accelerator section for the standard ID beamline case for the nominal parameter set. The boundary after the aperture at BPM 1 is a parallelogram, which in turn is modified by quadrupole QF, the aperture A2 and quadrupole QD. The phase space boundary consists of several segments, each of which is the consequence of an aperture cut. In particular, the top and right segments of the boundary at the dipole entrance can be

identified as the cut by the negative side of A1 and the positive side of A2, respectively. As particles with large horizontal offset in the dipole magnet receive less bending (see Figure 2), at the dipole exit the corner determined by these two segments is elongated. Particles inside this corner have large horizontal position and angle and are the ones that are likely to enter the photon beamline.

The exit of the sextupole magnet SD is the tracking endpoint. The trajectories downstream are simple straight lines since there is no magnetic field in the photon beamline. The top tip on the right-hand-side of the phase space boundary at the SD exit corresponds to a trajectory with the largest horizontal position and horizontal angle toward the experimental floor. If this trajectory is stopped by the negative side of a photon beamline aperture, then no other trajectories can pass beyond the aperture. In such a sense this trajectory is the most dangerous one, which we define as the *extreme ray*. At any photon beamline aperture, such as the safe endpoint or the ratchet wall aperture, the distance from the negative tip of the aperture to the extreme ray serves as a measure of the safety. This distance is defined as the *safety metric*. The extreme ray is stopped by an aperture if its safety metric is a negative number.

Particle tracking is based on the electron beam reference coordinate system for which the origins are the centers of SPEAR3 magnets. For the convenience of safety metric calculation, at the SD magnet exit, a coordinate transformation is performed to obtain coordinates in the photon beamline coordinate system.

4.2.3. The worst case

The shape of the final phase space boundary varies as the upstream control parameters change. However, the extreme ray can be defined as we do in the last section for a very large parameter range. The trajectory that grazes the positive tip of A2 with the largest angle coordinate θ will be the extreme ray since it receives the least inward bending from the dipole magnet, which dominates the behavior the trajectory downstream of A2. It might look possible for the rays represented by the far-left end of the top side of the phase space boundary at the QF exit (Figure 4) to supersede the extreme ray defined above since these rays have larger angle coordinates at the A2 aperture. However, the distance between the QF exit and the dipole center is only about 1.5 m, too short for such rays to catch up the extreme ray before the dipole further separate them. It is estimated and verified with tracking

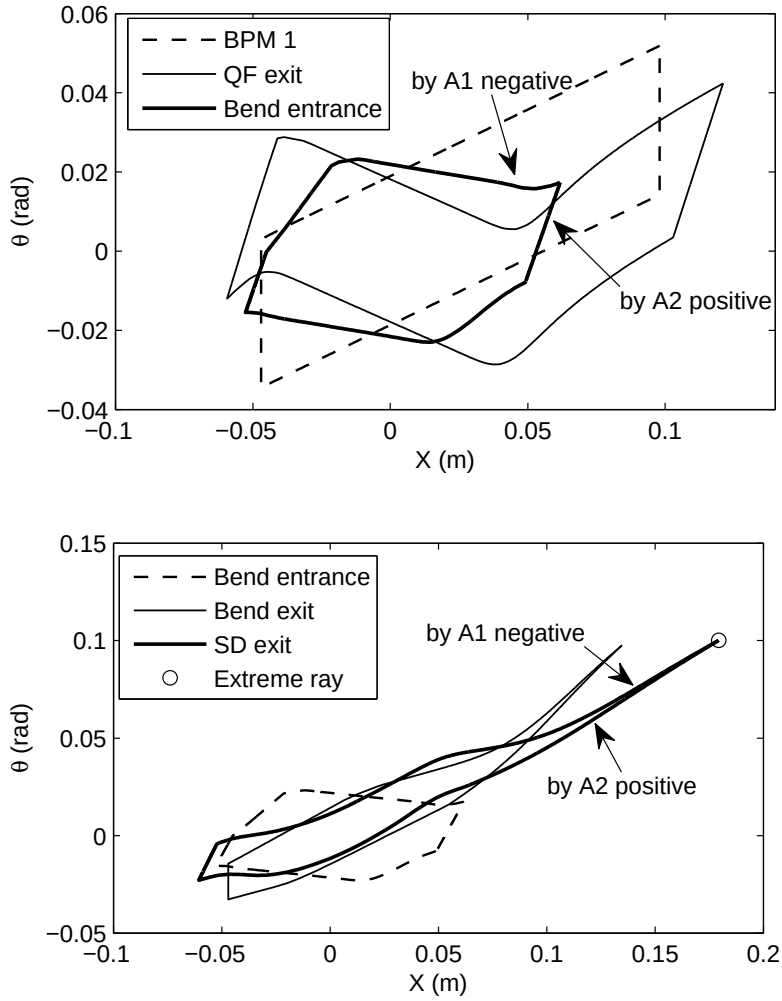

Figure 4: Phase space boundary at several locations for the standard ID beamline case for the nominal parameter set.

that the QF magnet needs to be 140% as strong as the power supply limit for that to happen. Since the magnetic field changes sign only in quadrupoles and the extreme ray passes through a definitive side (i.e., the positive side) in both quadrupoles (QF and QD), the magnetic field the extreme ray sees in all magnets does not change sign as the control parameters vary. Chang-

ing the strength of each magnet has a definitive effect to the extreme ray. In other words, the safety metric is monotonic with respect to each control parameter.

Therefore, when the allowed parameter space is reasonably chosen, the following two properties are expected to remain: (1) the trajectory defined by apertures A1 negative and A2 positive is the extreme ray; (2) the safety metric at the safe endpoint is monotonic with respect to any parameter. Within such a parameter space the largest safety metric (with the trajectory closest to the experimental floor) for the allowed range of a parameter always corresponds to the value at one of its two ends. This limit is called the worst-case value of the parameter. The case for all parameters at their corresponding worst-case values is referred to as the *worst case*, which has the largest safety metric among all allowed parameter sets. If the worst-case extreme ray is blocked by the negative side of an aperture at or upstream of the safe endpoint, so are all rays for all cases within the parameter space.

The worst-case safety metrics for the standard ID beamlines at the safe endpoint and the ratchet wall are given in Table 3 as examples. It should be noted that the BL 10 safe endpoint is the front-end mask, which is about 3 to 5 meters upstream of the safe endpoints of the other beamlines. The negative separation metrics indicate that all possible trajectories are intercepted by an aperture at or before the safe endpoint and the ratchet wall opening.

Table 3: The worst-case separation metric (in meter)

Beamline	safe endpoint	ratchet wall
BL 4	−0.165	−0.152
BL 5	−0.192	−0.165
BL 6	−0.242	−0.324
BL 7	−0.089	−0.193
BL 9	−0.086	−0.236
BL 10	−0.015	−0.244
BL 11	−0.164	−0.160

The monotonicity of the safety metric with respect to the the parameters can be easily tested by a multi-variable scan over the allowed parameter space. Simple elements, such as correctors and insertion device kicks may be exempted from the scan as their effect to the phase space is obvious.

5. The dipole beamline and special ID beamline cases

5.1. The dipole beamlines

The photon beam source point for all SPEAR3 dipole magnet is at 0.16 rad of the first bend magnet (total bending angle is $\pi/17$). The tracking setup is more complicated than the standard ID beamline case since more magnets are involved (Figure 5). But the same analysis approach is applicable. In this case the negative side of A2 aperture and the positive side of A3 aperture defines the extreme ray. The magnetic fields of the sextupole magnets do not cause large relative change of θ coordinate between the trajectories since they do not change sign on the middle plane. The QFC magnet would supersede the extreme ray with a trajectory that has negative position coordinate and large angle coordinate at its exit if it is sufficiently strong. However, the QFC magnet is not very efficient to that effect because the positive tip of the A3 aperture is further out (0.105 m from the reference orbit) than that of the A2 aperture, corresponding to the weak tail field of the magnet (Figure 3). It is shown by tracking that the QFC magnet needs to be at 170% of the power supply limit for the extreme ray to be re-defined. Similar to the standard ID beamline case, the extreme ray safety metric is monotonic with respect to the control parameters. Therefore we can define the worst case as the parameter set in which all parameters are at their corresponding worst-case values. The worst-case safety metric represent the most dangerous situation.

It was found that in the worst case, the extreme ray would pass beyond the safety endpoints. This is because the first dipole does not provide much separation (the photon beam source point is toward the end of the magnet) between the photon trajectory and the nominal electron trajectory and the extreme ray only passes through the weak tail field of the second dipole magnet. To control the hazard, SSRL installed electromagnetic clearing dipole magnet (ECD) at the front end of the dipole beamlines. The ECD magnet is designed to provide a 44 mrad kick for the 3 GeV beam. The design specification and measured field integral of the magnetic field are shown in Figure 6. In the tracking simulation the specified field profile is assumed. The phase space boundary at the ECD magnet in photon beamline coordinates for the worst case is shown in Figure 7. With the ECD magnets included, all dipole beamlines are safe with large safety margins.

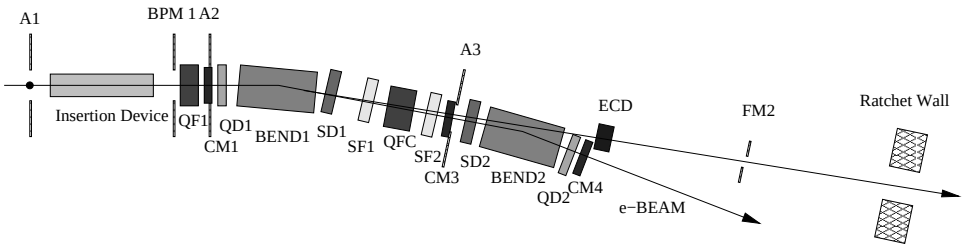

Figure 5: Layout for dipole beamlines.

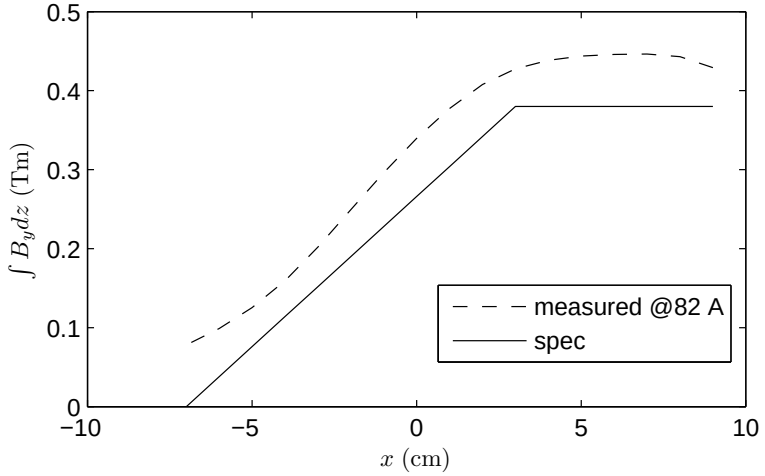

Figure 6: The specification and measurement of the ECD magnetic field integral.

5.2. Beamline 12 and Beamline 13

Beamline 12 and Beamline 13 are two special cases for the top-off safety analysis. Both cases involve the matching cells for which the bend magnets are only 3/4 of the normal bends in lengths and bending angles. The layout for Beamline 13 is similar to the standard ID cases (Figure 8 bottom plot). The same type of magnets and apertures appear in the same sequence. In addition to a weaker dipole magnet, another difference is that the length of the insertion device drift space is longer. The extreme ray defined by A1 negative and A2 positive would pass beyond the safe endpoint (which is the collimator). However, the positive side of the FM1 aperture cuts the top-right corner of the phase space boundary and re-defines the extreme ray

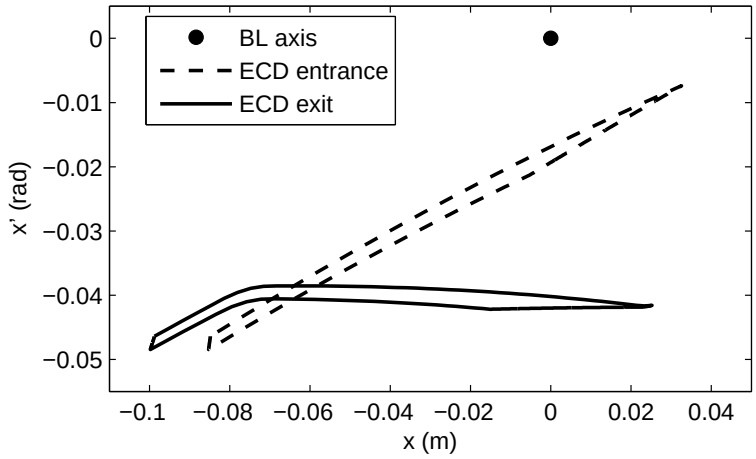

Figure 7: The phase space boundary (in photon beamline axis) at the entrance and the exit of the ECD magnet for the worst case.

(Figure 9). The new extreme ray is safe for the safe endpoint and the ratchet wall opening with a reasonable safety margin.

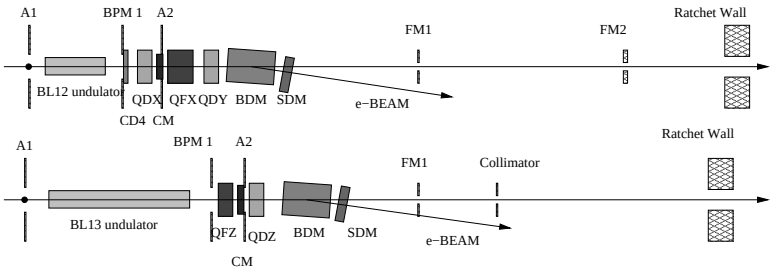

Figure 8: Layout for BL12 (top) and BL13 (bottom).

The Beamline 12 undulator is in a chicane straight section. The tracking setup is different from the standard ID beamlines. In addition to a weaker bend magnet, there is a 8 mrad chicane dipole that follows the undulator. To avoid interlocking the chicane magnet, its worst-case bending angle is set to zero. There is a quadrupole triplet with one focusing and two defocusing quadrupole magnets before the bend. The length of the chicane straight section is shorter than a standard one. These factors make the extreme ray determined by the A1 and A2 apertures point further toward the SSRL

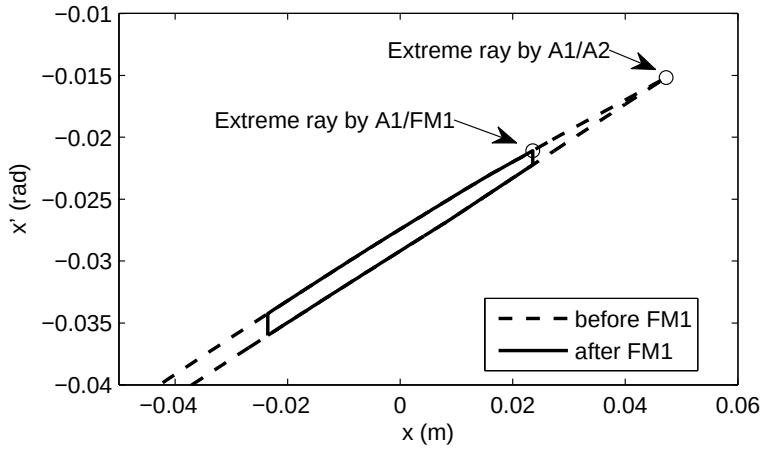

Figure 9: The phase space boundary at the front-end fixed mask for the Beamline 13 worst case.

experimental floor. We also rely on the front end fixed mask (FM1) to trim the phase space boundary. The new extreme ray defined by A1 and FM1 is safe for both the safe endpoint and the ratchet wall.

For Beamlines 12 and 13, because of the increased distance and the number of elements between the two limiting apertures, we took the precaution to perform multi-variable scans to verify the monotonicity of the safety metric with respect to the parameters. The results confirmed our analysis.

6. Conclusions

Radiation hazard control is important for top-off operation. A prerequisite of top-off is the determination and implementation of an operational parameter envelope within which no injected electron can pass beyond certain predetermined safe endpoints in the photon beamlines. At SSRL, the forward tracking approach is taken to address the problem. For each beamline, particles are launched from the beginning of the preceding straight section and tracked to the safe endpoint. Compared to approaches previously reported [4, 2], our approach may be simpler in several aspects. First, only particles on a closed 2D phase space boundary are tracked because the Liouville's theorem dictates that no particles inside such a boundary can surpass all particles on the boundary and obtain extreme values in either position or

angle coordinates. Second, for each parameter set, an extreme ray is defined to represent the most dangerous trajectory and a numeric number, the safety metric, is used as a measure of safety, which simplifies the interpretation of tracking results. Third, we identify the two limiting apertures that define the extreme ray and prove that the safety metric is monotonic with respect to any controlled parameter in the parameter space allowed for top-off operation. This fact allows us to define a worst-case value for any parameter and the overall worst-case parameter set for the entire parameter space. Identifying the limiting apertures, the effect of each parameter on the safety metric and the worst case gives us a clear picture of the safety scenario, which is crucial for the determination of interlock limits and for future addition of beamlines.

Acknowledgment

The study is supported by DOE Contract No. DE-AC02-76SF00515.

References

[1] L. Emery, M. Borland, Top-up operation experience at the Advanced Photon Source, Proceedings of PAC'99, New York (1999).

[2] H. Nishimura, *et al.*, Nucl. Instrum. Methods A **608** (2009), 2-18.

[3] J. Liu, *et al.*, SLAC RP-07-23, November 2007.

[4] M. Borland, L. Emery, Tracking studies of top-up safety for the Advanced Photon Source, Proceedings of PAC'99, New York (1999).

[5] R. Hettel, *et al.*, SPEAR3 upgrade project: the final year, Proceedings of PAC'03, Portland, Oregon (2003).

[6] J. Schmerge, *et al.*, SSRL AP-note-007, December 2007.

[7] X. Huang, SSRL AP-note-015, April 2009.

[8] A. Terebilo, Accelerator modeling with Matlab Accelerator Toolbox, Proceedings of PAC'01, Chicago (2001)